

LETTER TO THE EDITOR

SOME INDICATIONS OF LIQUID-GAS PHASE TRANSITION IN
ELECTRON-INDUCED FRAGMENTATION OF ^{197}Au NUCLEI

G. E. MARKARYAN

*Yerevan Physics Institute, 375036 Yerevan, Armenia
E-mail address: garik@mail.yerphi.am*

Received 21 October 2006; Revised manuscript received 25 April 2007
Accepted 16 May 2007 Online 21 June 2007

The energy spectra and fragment yields ($5 < Z_F < 10$) obtained in 1.5–4.5 GeV $e + ^{197}\text{Au}$ inclusive reactions are analysed. Based on the observed correlation between a decrease in the fragment yields and an increase in the fragment Coulomb energy with the fragment charge, temperatures of the fragmenting system are derived. It is shown that the fragment yields exhibit the feature of thermal scaling in accordance with the Fisher's droplet model. By using this model, values for the zero temperature surface energy coefficient, $c_0 = 11.8 \pm 0.8$ MeV, the critical exponent, $\sigma = 0.56 \pm 0.03$, as well as estimation of the critical temperature, $T_c \approx 18$ MeV are obtained. The obtained results argue in favour of nuclear liquid-gas phase transition in these electron-induced reactions.

PACS numbers: 25.30.-c, 25.30.Rw

UDC 539.172

Keywords: electron-induced fragmentation, fragment cross sections, Coulomb energies, thermal scaling, Fisher's droplet model, liquid-gas phase transition

For the two last decades, the intermediate-mass fragment (IMF, $3 < Z_F < 20$) emission in reactions induced on nuclei by energetic projectiles has been the subject of both intense experimental and theoretical study [1–25]. In particular, the interest in this study has been stimulated by a possible link between multiple productions of these fragments (multifragmentation) and the liquid-gas phase transition in the excited nuclear matter [1–19]. The physical reason for such a possibility is based on the similarity between the Van der Waals and nucleon-nucleon forces in their general features of short-range repulsion followed by attraction. The search for unambiguous signatures of such a transition has been and remains one of the active lines of investigations in current nuclear physics. In these investigations, much at-

tention has recently been paid to nuclear fragmentation induced by light relativistic particles. These projectiles offer some advantages, the main of which are: (i) the fragments are emitted only from a source related to a target nucleus; (ii) pure thermal excitation of the nucleus in collisions with such projectiles facilitates a study of thermodynamic processes leading to the fragment production (the dynamic effects due to compression, rotation and shape distortion of the nucleus are negligible). Several elaborated exclusive experiments on fragmentation of Au nuclei by GeV hadrons (π , p) have been performed recently and definite signatures of a nuclear liquid-gas phase transition have been found [14–19]. For instance, in the study of the $\pi^- + {}^{197}\text{Au}$ reaction at 8.0 GeV/c by ISiS collaboration, various scaling laws in the IMF yields have been observed. These scaling laws, in particular the thermal scaling exhibiting features inherent to Fisher’s droplet model [26], are considered to be a strong argument in favour of a nuclear liquid-gas phase transition [15–16]. Although such thermal scaling has been observed for the multifragmentation events from the highly excited systems, it has been shown recently that low-energy compound nucleus emission of IMFs also scale according to Fisher’s model and can be simultaneously fit with the much higher-energy ISiS multifragmentation data [17]. In view of this, it would also be of interest, in terms of Fisher’s droplet model, to examine IMF emission in reactions induced on nuclei, for instance, by GeV electrons. It should be noted that energetic electrons, like other light relativistic projectiles, are well suited for investigations of thermal aspects of nuclear fragmentation, but, unfortunately, very little information is available on electron-induced fragmentation of nuclei [20–21]. In our previous work [20] we presented an analysis of the IMF ($4 < Z_F < 10$) energy spectra obtained at angles of 50° , 90° and 120° in the study of the 1.5–4.5 GeV $e + {}^{197}\text{Au}$ inclusive reaction at the Yerevan synchrotron. The main results of the previous analysis are: (i) the fragments are isotropically emitted from some moving source which is essentially smaller than the target nucleus; (ii) the fragment energy spectra exhibit Maxwell-Boltzmann-like shape; (iii) the Coulomb peaks of the spectra are shifted towards higher energies for larger fragment charge and slightly towards lower kinetic energies for larger incident electron energy; (iv) the values for the source velocity, the fragment Coulomb energies and the fragment differential cross sections at the measured angles have also been derived from the data.

In this letter, based on the results of Ref. [20], an analysis of the fragment ($5 < Z_F < 10$) emission in the same $e + {}^{197}\text{Au}$ reaction is performed with the aim of finding some indications of a liquid-gas phase transition, in particular, a possible manifestation of thermal scaling in the fragments yields and interpretation of these yields by Fisher’s droplet model [15–16, 26]. The analysis begins with a qualitative examination of the dependence of the fragment energy spectra on the fragment charge. As a typical example, Fig. 1a shows the laboratory energy spectra for Be up to Mg fragments emitted at 90° in the reaction induced by 4.5 GeV electrons. In this figure, the fragment double differential cross sections are multiplied by some factors for better visualization of the spectra. It is of interest, however, to look at the same spectra when they are plotted without using these factors. Such a plot of the spectra is shown in Fig. 1b.

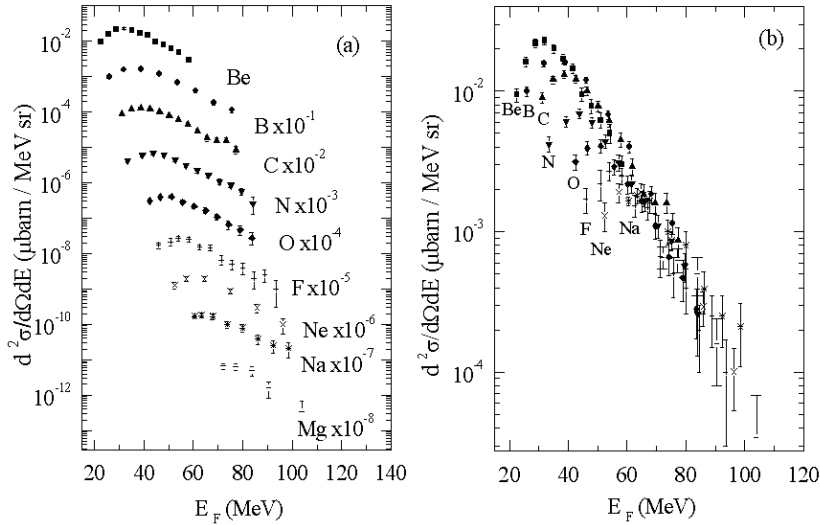


Fig. 1. Fragment energy spectra at 90° in the laboratory frame for 4.5 GeV electron-induced reactions on gold: a) the fragment double-differential cross sections are multiplied by the factors shown in the figure; b) the same spectra are plotted without using these factors.

As can be seen from Fig. 1b, the high-energy portions of the fragment spectra nearly overlap and, for the heavier fragments, this feature is observed just above the corresponding Coulomb-like peaks. Moreover, one can see a nearly exponential fall of these peaks with the fragment charge. A similar picture is observed at the other measured angles and incident energies. It should be noted that a similar overlapping of high-energy parts of the (C–Ar) fragment spectra was observed earlier by Poskanzer et al. in their study of the 5.5 GeV $p + {}^{238}\text{U}$ reaction [22]. At first sight, such an overlapping, i.e. an approximate equality of the laboratory double differential cross sections in high-energy parts of the spectra for different fragments, may seem to be surprising. To understand the reason of this effect, the obtained fragment spectra [20] were transformed from the laboratory system into the system associated with the fragment-emitting source. In performing this transformation, the obtained fragment Coulomb energies [20] were subtracted from the corresponding fragment kinetic energies in the laboratory frame thus accounting for thermal character of the fragment emission in the source frame [23]. As an illustration, Fig. 2 shows the results of this transformation for the fragment spectra presented in Fig. 1b. Similar diagrams are observed for the other measured angles and incident energies.

It is seen from Fig. 2 that after such a transformation, there is no overlap of the spectra for fragments with $5 < Z_F < 10$, the spectra are nearly identical in shape, and the maxima of the spectra are located approximately at the same kinetic energy. These features are typical for the emission of fragments from a common heated source [20, 24–25]. Thus, from comparison of the spectra shown

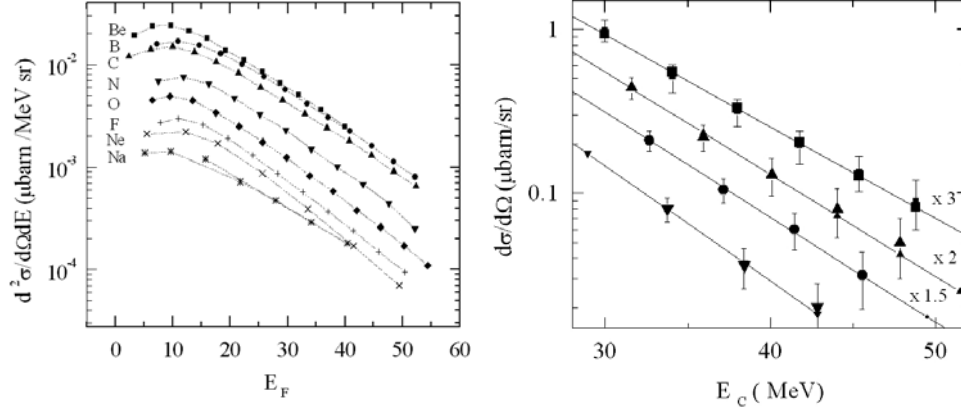


Fig. 2 (left). The same spectra as in Fig. 1b are shown after their transformation into the source frame according to the procedure described in the text. Dotted lines are drawn to guide the eye.

Fig. 3. The dependence of the fragment cross sections $d\sigma/d\Omega$ at 90° on the corresponding fragment Coulomb energies: $E_e = 4.5$ GeV (\blacksquare), the cross sections of the fragments (C–Na) are multiplied by the factor 3; $E_e = 3$ GeV (\blacktriangle), the cross sections of the fragments (C–Ne) are multiplied by the factor 2; $E_e = 2$ GeV (\bullet), the cross sections of the fragments (C–F) are multiplied by the factor 1.5; $E_e = 1.5$ GeV (\blacktriangledown), the cross sections of the fragments (C–O). Solid lines represent the fit described in the text.

in Figs. 1b and 2, one can conclude that the observed overlapping of the spectra in the laboratory frame may arise from some correlation between a decrease of the fragment yield and an increase in the Coulomb energy with the fragment charge. Taking into account the mentioned nearly exponential fall of the maxima of the spectra with the fragment charge (Fig. 1), one can expect an exponential character of this correlation. In Fig. 3, the fragment ($Z_F > 5$) differential cross sections $d\sigma/d\Omega$ at 90° are plotted as a function of the corresponding fragment Coulomb energies, E_C , which have been obtained from the fit of the fragment energy spectra with Maxwell-Boltzmann-type expression [20], and presented for all incident electron energies E_e in Table 1. From Fig. 3, one can see a nearly exponential fall of the cross sections with the fragment Coulomb energy.

TABLE 1. Values of the fragment Coulomb energies, E_C , obtained from the fit of the fragment energy spectra with Maxwell-Boltzmann-type expression [20].

E_e (GeV)	$Z_F = 6$	7	8	9	10	11
	E_C (MeV)					
1.5	33.8	38.4	42.9			
2	32.7	37.2	41.5	45.6		
3	31.6	35.9	40.1	44.1	47.9	
4.5	30.5	34.7	38.7	42.5	46.2	49.7

The dependence of the fragment cross sections on Coulomb energy (Fig. 3) were fitted by the equation

$$d\sigma/d\Omega = N \exp(-E_C/T), \quad (1)$$

where N is a normalization constant, E_C is the fragment Coulomb energy, and T is a free parameter. The values for the parameter T obtained from this fit are presented in Table 2 and the corresponding fitting curves are shown in Fig. 3. It should be noted that, due to the observed isotropic fragment emission in the source frame and a weak angular dependence of the fragment yields in the laboratory frame [20], one can use in this analysis the fragment yields (or cross sections) at a given angle, in particular, at 90° .

TABLE 2. The values for the parameter T obtained from the fit of the fragment cross sections at 90° with the expression $d\sigma/d\Omega = N \exp(-E_C/T)$.

E_e (GeV)	1.5	2	3	4.5
T (MeV)	6.3 ± 0.4	6.8 ± 0.3	7.3 ± 0.3	7.7 ± 0.3

From Table 2, one can see some increase of the parameter T with the incident energy. On the other hand, as can be seen from Table 1 and Fig. 3, the obtained fragment Coulomb energies slightly decrease with the incident electron energy. Consequently, the fragment Coulomb energies should decrease with the parameter T . Based on these indications, and taking also into account the form of the fitting equation (1), it is assumed that the extracted values for the parameter T can be taken as temperatures of the fragment emitting source. This assumption makes it possible, for each measured fragment, to examine dependence of its yield on the inverse temperature $1/T$, i.e. to examine the so called Arrhenius plots [16]. Figure 4 shows such plots for C, N, O, and F fragments.

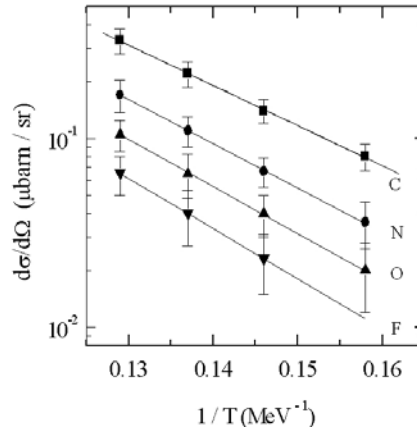


Fig. 4. The cross sections $d\sigma/d\Omega$ of the fragments (C–F) at 90° plotted against the inverse temperature $1/T$ (Arrhenius plots). Solid lines represent the fit described in the text.

As can be seen, for each considered fragment, a linear dependence of the logarithm of the fragment cross section $d\sigma/d\Omega$ on the inverse temperature $1/T$ is observed. Such dependence is characteristic of thermal scaling, which refers to the feature that the average fragment yield $\langle N \rangle$ behaves as a Boltzmann factor $\langle N \rangle \propto \exp(-B/T)$ as a function of temperature T , where B is the one-fragment production barrier [15, 16].

As has been shown by Elliot et al. [15, 16], the feature of thermal scaling is inherent to Fisher's droplet model [26], according to which the yield of the fragment of size A is given by

$$Y(A) = Y_0 A^{-\tau} \exp(A\Delta\mu/T - cA^\sigma/T), \quad (2)$$

where Y_0 is a normalization constant, τ is the topological critical exponent, $\Delta\mu = \mu_g - \mu_l$ is the difference of chemical potentials of gaseous and liquid phases, c is the surface free energy density which depends on temperature, σ is the critical exponent related to the ratio of the dimensionality of the surface to that of the volume and T is the temperature of the fragmenting system. By using the parameterization $c = c_0(1 - T/T_c)$ [15, 16, 26], where c_0 is the zero temperature surface energy coefficient and T_c is the critical temperature, Eq. (2) can be written as follows

$$Y(A) = Y_0 A^{-\tau} \exp(c_0 A^\sigma/T_c) \exp(-(c_0 A^\sigma - A\Delta\mu)/T). \quad (3)$$

It is seen from (3) that for a given fragment, its yield as a function of T can be written as follows

$$Y(A) \propto \exp(-(c_0 A^\sigma - A\Delta\mu)/T). \quad (4)$$

Thus, expression (4) clearly shows the feature of thermal scaling in Fisher's model. In the region of phase coexistence ($\Delta\mu = 0$), expression (4) is reduced to

$$Y(A) \propto \exp(-c_0 A^\sigma/T), \quad (5)$$

with a barrier $B = c_0 A^\sigma$ (the cost to create the surface of a fragment of size A) [16].

Since the dependence of the cross sections on the inverse temperature for fragments (C, N, O, and F) obtained in this work exhibit the feature of thermal scaling (see Fig. 4), it would be of interest to make comparison with the result inherent to Fisher's model (5). The comparison was performed as follows. First, this dependence for each fragment (C, N, O, and F) has been fitted using the equation $d\sigma/d\Omega = N_1 \exp(-B/T)$, where N_1 is a normalization constant, B is a free parameter, and T is the temperature. In performing these fits, temperatures, T , were fixed at values given in Table 2. The fits yielded the following values for the barrier B : 49.2 ± 0.7 , 53.9 ± 0.6 , 57.1 ± 0.8 , 61.1 ± 0.7 MeV for fragments C, N, O, and F, respectively. In Fig. 5, these values for B are plotted against the fragment mass number A and one can see that such a dependence of B on A can be approximated by a power law.

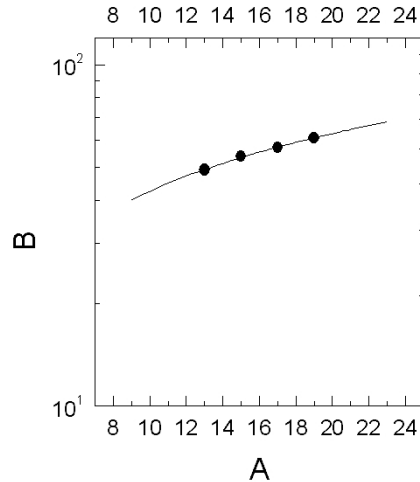


Fig. 5. The obtained values for the barrier B plotted against the fragment mass number A . The solid line represents the power-law fit described in the text.

Taking this into account and assuming $\Delta\mu = 0$, this dependence of B on A has been fitted using the equation $B = c_0 A^\sigma$ [15] and the following values for c_0 and σ have been obtained: $c_0 = 11.8 \pm 0.8$ MeV, $\sigma = 0.56 \pm 0.03$. It should be noted that in performing this fit as well as in plotting B vs. A , the fragment mass number A was determined by the equation $A = 2Z + 1$, which accounts for the more abundant yield of neutron-excess isotopes of the fragments in reactions induced on heavy targets [2, 3, 22]. The derived values for c_0 and σ are in the range of the results determined in other works. For example, the analysis of Au data by the EOS Collaboration yielded $c_0 = 6.8 \pm 0.5$ MeV and $\sigma = 0.68 \pm 0.03$ [15], whereas the analysis of the 8.0 GeV/ c $\pi^- + ^{197}\text{Au}$ data of the ISIS Collaboration yielded $c_0 = 18.3 \pm 0.5$ MeV and $\sigma = 0.54 \pm 0.01$ [16]. It should also be noted, that the value $\sigma = 0.56 \pm 0.03$ derived in this work is close (as in Refs. [15] and 16)) to 2/3 of what one can expect for a three dimensional spherical system [16]. In addition, an attempt was made to estimate the critical temperature, T_c , by analysing the obtained fragment charge distributions [20] in terms of Fisher's droplet model [15–16, 26]. As an illustration, Fig. 6 shows these charge distributions at 90° .

In performing the present analysis, the obtained values for c_0 and σ as well as the critical exponent $\tau = 2$ were used. This analysis of the fragment charge distributions for all incident electron energies (1.5–4.5 GeV) yielded nearly the same estimation of the critical temperature, $T_c \approx 18$ MeV. It should be noted that this estimate is in the range of values ($\approx 5 - 20$ MeV) obtained for the critical temperature in the experimental and theoretical works [2–7, 15, 16, 19]. For instance, this estimation is larger than the values for T_c (6–8 MeV) obtained in Refs. [15, 16], but it is consistent with the value $T_c \approx 20$ MeV obtained from the analysis of the 8.1 GeV $p + ^{197}\text{Au}$ reaction measured by the FASA Collaboration [19]. Finally, by using this estimation of the critical temperature, the values for the control parameter $\epsilon = (T_c - T)/T_c$ have been determined. The results are shown in Fig. 7 as a plot of

the scaled cross sections $(d\sigma/d\Omega)/A^{-\tau}$ against the scaled temperature $A^\sigma\epsilon/T$ [16] for the fragments with $Z > 5$.

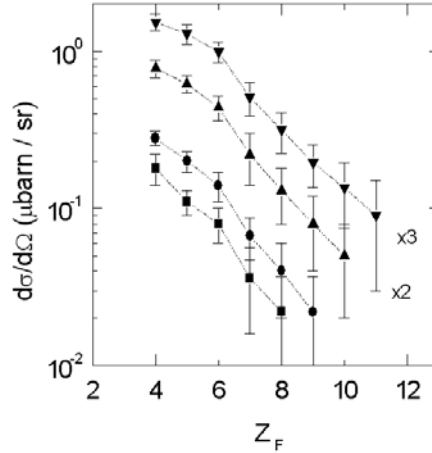


Fig. 6. Charge distributions of the fragments ($Z_F \geq 4$, $\theta = 90^\circ$) obtained in 1.5–4.5 GeV $e + \text{Au}$ reactions: $E_e = 1.5$ GeV (■), $E_e = 2$ GeV (●), $E_e = 3$ GeV (▲), the cross sections of the fragments are multiplied by the factor 2, $E_e = 4.5$ GeV (▼), the cross sections of the fragments are multiplied by the factor 3. Broken lines are drawn to guide the eye.

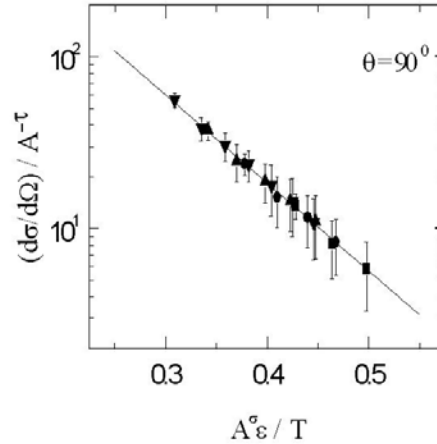


Fig. 7. The dependence of the scaled fragment cross sections $d\sigma/d\Omega/A^{-\tau}$ ($Z_F > 5$) on the scaled temperature ($A^\sigma\epsilon/T$): $E_e = 1.5$ GeV (■), $E_e = 2$ GeV (●), $E_e = 3$ GeV (▲), $E_e = 4.5$ GeV (▼). The solid line represents an exponential fit to the scaled data.

As can be seen, the scaled cross sections versus the scaled temperature, for all incident energies and considered fragments, are located on a single line. The slope of this line, obtained from an exponential fit of the scaled data, is $\approx 11.9 \pm 0.4$

MeV and this value almost coincides with $c_0 = 11.8 \pm 0.8$ MeV derived from the power-law fit of the obtained barriers B . Such a behaviour of the scaled data is in agreement with Fisher's droplet model [15, 16, 26].

In summary, the above analysis of the energy spectra and the fragment ($5 < Z_F < 10$) yields obtained in the 1.5–4.5 GeV $e + {}^{197}\text{Au}$ inclusive reactions shows: (i) that the observed overlapping of high energy parts of the spectra can be understood in terms of a correlation between a decrease of the fragment yield and an increase in the fragment Coulomb energy with the fragment charge, (ii) that based on this correlation, temperatures of the fragmenting system are derived, (iii) that the fragment yields exhibit the feature of thermal scaling which is consistent with that inherent to Fisher's droplet model, (iv) that the obtained values for the zero temperature surface energy coefficient c_0 and the critical exponent σ , as well as estimation of the critical temperature T_c are in the range of the accepted values quoted in literature, (v) that the scaled fragment yields versus the scaled temperature are located on a single line in accordance with the Fisher's droplet model. Thus, the obtained results indicate adherence of the fragment yields to Fisher's droplet model and argue in favour of the nuclear liquid-gas phase transition in these electron-induced reactions on ${}^{197}\text{Au}$ nuclei.

The author wishes to thank H. A. Vartapetyan, A. M. Sirunyan and H. V. Badalyan for their interest in this work.

References

- [1] J. E. Finn et al., Phys. Rev. Lett. **49** (1982) 1321.
- [2] A. S. Hirsh, A. Bujak, J. E. Finn, L. J. Gutay, R.W. Minich, N. T. Porile, R. P. Sharenberg and B. C. Stringfellow, Phys. Rev. C **29** (1984) 508.
- [3] N. T. Porile et al., Phys. Rev. C **39** (1989) 1914.
- [4] A. D. Panagiotou, M. W. Curtin, H. Toki and D. K. Scott, Phys. Rev. Lett. **52** (1984) 496.
- [5] A. D. Panagiotou, M. W. Curtin and D. K. Scott, Phys. Rev. C **31** (1985) 55.
- [6] A. L. Goodman, J. I. Kapusta and A. Z. Mekjian, Phys. Rev. C **30** (1984) 851.
- [7] L. P. Csernai and J. I. Kapusta, Phys. Rep. **131** (1986).
- [8] V. V. Avdeichikov et al., Yad. Fiz. **48** (1988) 1736.
- [9] S. J. Yenello et al., Phys. Rev. C **48** (1993) 10.
- [10] J. Hufner, Phys. Rep. **125** (1985) 129.
- [11] W. G. Lynch, Ann. Rev. Nucl. Part. Sci. **37** (1987) 493.
- [12] J. Richert and R. Wagner, Phys. Rep. **350** (2001) 1.
- [13] V. A. Karnaukhov et al., Yad. Fiz. **62**(1999) 272.
- [14] T. Lefort et al., Phys. Rev. C **64** (2001) 064603.
- [15] J. B. Elliott et al., Phys. Rev. Lett. **85** (2000) 1194.
- [16] J. B. Elliott et al., Phys. Rev. Lett. **88** (2002) 042701.
- [17] L. G. Moretto, J. B. Elliot, L. Phair and G. J. Wozniak, LBNL-51306

- [18] S. P. Avdeev et al., *Yad. Fiz.* **64** (2001) 1628.
- [19] V. A. Karnaukhov et al., *Phys. Rev. C* **67** (2003) 011601.
- [20] G. E. Markaryan, G. M. Aivazyan, H. V. Badalyan, D. M. Beglaryan and H. G. Zohrabyan, *J. Phys. G: Nucl. Part. Phys.* **25** (1999) L101.
- [21] S. Liberto et al., *Nucl. Phys. A* **296** (1978) 519.
- [22] A. M. Poskanzer, G. W. Butler and E. K. Hide, *Phys. Rev. C* **3** (1971) 882.
- [23] D. J. Fields, W. B. Lynch, C. B. Chitwood, C.K. Gelbke, M. B. Tsang, H. Utsunomiya and J. Aichelin, *Phys. Rev. C* **30** (1984) 1912.
- [24] A. Z. Mekjian, *Phys. Rev. C* **17** (1978) 1051.
- [25] S. Das Gupta and A. Z. Mekjan, *Phys. Rep.* **72** (1981) 131.
- [26] M. E. Fisher, *Physics (N. Y.)* **3** (1967) 255.

NEKI POKAZATELJI FAZNOG PRIJELAZA TEKUĆINA-PLIN U RAZBIJANJU JEZGRI ^{197}Au ELEKTRONIMA

Analiziramo energijske spektre i prinose izbačenih jezgri ($5 < Z_F < 10$) u inkluzivnim reakcijama $1.5 - 4.5 \text{ GeV } e + ^{197}\text{Au}$. Na osnovi opaženih korelacija smanjenja prinosa izbačenih jezgri i povećanja Coulombove energije s nabojem izbačenih jezgri izvodimo temperature udarenog sustava. Opažamo da prinosi izbačenih jezgri pokazuju toplinsko sumjeravanje u skladu s Fisherovim modelom kapljice. Primjenom tog modela izveli smo koeficijent površinske energije na temperaturnoj nuli, $c_0 = 11.8 \pm 0.8 \text{ MeV}$, i kritični eksponent, $\sigma = 0.56 \pm 0.03$, te ocijenili kritičnu temperaturu, $T_c \approx 18 \text{ MeV}$. Postignuti rezultati ukazuju na nuklearni fazni prijelaz tekućina-plin u tim reakcijama izazvanim elektronima.